Novel Role of the IGF-1 Receptor in Endothelial Function and Repair

Studies in Endothelium-Targeted IGF-1 Receptor Transgenic Mice

Helen Imrie,[1] Hema Viswambharan,[1] Piruthivi Sukumar,[1] Afroze Abbas,[1] Richard M. Cubbon,[1] Nadira Yuldasheva,[1] Matthew Gage,[1] Jessica Smith,[1] Stacey Galloway,[1] Anna Skromna,[1] Sheik Taqweer Rashid,[1] T. Simon Futers,[1] Shouhong Xuan,[2] V. Kate Gatenby,[1] Peter J. Grant,[1] Keith M. Channon,[3] David J. Beech,[1] Stephen B. Wheatcroft,[1] and Mark T. Kearney[1]

We recently demonstrated that reducing IGF-1 receptor (IGF-1R) numbers in the endothelium enhances nitric oxide (NO) bioavailability and endothelial cell insulin sensitivity. In the present report, we aimed to examine the effect of increasing IGF-1R on endothelial cell function and repair. To examine the effect of increasing IGF-1R in the endothelium, we generated mice overexpressing human IGF-1R in the endothelium (human IGF-1R endothelium-overexpressing mice [hIGFREO]) under direction of the Tie2 promoter enhancer. hIGFREO aorta had reduced basal NO bioavailability (percent constriction to N^G-monomethyl-L-arginine [mean (SEM) wild type 106% (30%); hIGFREO 48% (10%)]; $P < 0.05$). Endothelial cells from hIGFREO had reduced insulin-stimulated endothelial NO synthase activation (mean [SEM] wild type 170% [25%], hIGFREO 58% [3%]; $P = 0.04$) and insulin-stimulated NO release (mean [SEM] wild type 4,500 AU [1,000], hIGFREO 1,500 AU [700]; $P < 0.05$). hIGFREO mice had enhanced endothelium regeneration after denuding arterial injury (mean [SEM] percent recovered area, wild type 57% [2%], hIGFREO 47% [5%]; $P < 0.05$) and enhanced endothelial cell migration in vitro. The IGF-1R, although reducing NO bioavailability, enhances in situ endothelium regeneration. Manipulating IGF-1R in the endothelium may be a useful strategy to treat disorders of vascular growth and repair. ***Diabetes* 61:2359–2368, 2012**

Insulin-resistant type 2 diabetes characterized by perturbation of the insulin/IGF-1 system is a multisystem disorder of nutrient homeostasis, cell growth, and tissue repair (1). As a result, type 2 diabetes is a major risk factor for the development of a range of disorders of human health, including occlusive coronary artery disease (2), peripheral vascular disease (3), stroke (4), chronic vascular ulcers (5), proliferative retinopathy (6), and nephropathy (7). A key hallmark of these pathologies is endothelial cell dysfunction characterized by a reduction in bioavailability of the signaling radical nitric oxide (NO). In the endothelium, insulin binding to its tyrosine kinase receptor stimulates release of NO (8). Insulin resistance at a whole-body level (9,10) and specific to the endothelium (11) leads to reduced bioavailability of NO, indicative of a critical role for insulin in regulating NO bioavailability.

The insulin receptor (IR) and IGF-1 receptor (IGF-1R) are structurally similar—both composed of two extracellular α and two transmembrane β subunits linked by disulfide bonds (12). As a result, IGF-1R and IR can heterodimerize to form insulin-resistant hybrid receptors composed of one IGF-1R-αβ complex and one IR-αβ subunit complex (13,14). We recently demonstrated that reducing IGF-1R (by reducing the number of hybrid receptors) enhances insulin sensitivity and NO bioavailability in the endothelium (15). To examine the effect of increasing IGF-1R specifically in the endothelium on NO bioavailability, endothelial repair, and metabolic homeostasis, we generated a transgenic mouse with targeted overexpression of the human IGF-1R in the endothelium (hIGFREO).

RESEARCH DESIGN AND METHODS

Generation of hIGFREO mice. To overcome the limitations of random and multiple copy insertion sites seen in standard transgenics, we used the hypoxanthine phosphoribosyl transferase (*Hprt*) targeting system (Genoway; see ref. 16) to generate genetically modified embryonic stem (ES) cells. This approach uses homologous recombination to target a single copy of a transgene (in this case, the human *IGF-1r*), driven by a promoter (in this case, the Tie2 promoter), into the *Hprt* locus on the X chromosome. The model was developed with E15Tg2a (E14) cells derived from the strain 129P2/OiaHsd (12901a). In E14 cells, 35 kb of the *Hprt* gene encompassing the 5′ untranslated region up to intron 2 is deleted. The *Hprt* gene encodes a constitutively expressed housekeeping enzyme involved in the synthesis of purines from the degradation products of nucleotide bases (salvage pathway). Cells normally synthesize purines by the salvage and de novo pathways. In *Hprt*-deleted cell lines, only the de novo pathway is functional, enabling the cells to grow in classical medium. However, in the presence of the aminopterin drug, the de novo pathway is blocked. As a result, *Hprt*-deleted cells die in hypoxanthine-aminopterin-thymidine (HAT) media (containing HAT substrates). The targeted insertion of a transgenic cassette in E14 ES cells with a functional *Hprt* gene rescues these cells, which can then be selected using HAT media to identify ES cells showing the correct targeting event. ES cells with the correct insertion can be selected by virtue of their expression of *Hprt* and their ability to grow in HAT medium. Numerous studies have shown that the functional properties of the *Hprt* locus protect transgenic constructs inserted in this region against gene silencing and positional or methylation effects. Furthermore, tissue-specific promoters including Tie2 (17) inserted into the *Hprt* locus maintain their expression properties.

Vector construction. Endothelium-specific transgene expression was achieved using the mouse Tie2 promoter and intronic enhancer as previously

From the [1]Division of Cardiovascular and Diabetes Research, Multidisciplinary Cardiovascular Research Centre, University of Leeds, Leeds, U.K.; the [2]Department of Genetics and Development, Columbia University, New York, New York; and the [3]University of Oxford, British Heart Foundation Centre of Research Excellence, Oxford, U.K.
Corresponding author: Mark T. Kearney, m.t.kearney@leeds.ac.uk.
Received 25 October 2011 and accepted 18 April 2012.
DOI: 10.2337/db11-1494
This article contains Supplementary Data online at http://diabetes.diabetesjournals.org/lookup/suppl/doi:10.2337/db11-1494/-/DC1.

See accompanying commentary, p. 2225.

described (11,18). To reduce the size of the transgene, the minimal enhancer sequence (core enhancer) was inserted into the final construct. This sequence has been shown to confer a uniform and high level of expression of LacZ reporter gene in endothelial cells in vivo (17). The targeting vector was obtained by inserting human IGF-1R cDNA (a gift from Dr. R. Baserga, Jefferson University) (19) into the pHHNS plasmid (11,18), comprising the murine Tie2 promoter, *LacZ* cDNA, and SV40 polyA signal and a 10-kb intronic enhancer from the murine Tie2. The final transgenic vector (Fig. 1*A*), consisting of Tie2 promoter, human IGF-1R cDNA, SV40 polyadenylation site, and core enhancer, was then inserted into an *Hprt* targeting vector using standard cloning. The final targeting vector had the following features: *1*) homology arms isogenic with E14 ES cells favoring homologous recombination; *2*) symmetrical homology arms (5′ short arms: 3.8 kb, 3′ long arm: 3.7 kb); *3*) transgenic cassette expressing the human IGF-1R cDNA under control of the short form of the Tie2 promoter; and *4*) wild-type *Hprt* sequences to reconstitute the *Hprt* gene in the E14 ES cells. In ES cells, this process was highly successful, with three clones selected for blastocyst injection. The 5′ and 3′ targeting events were unambiguously confirmed by Southern blot analysis. These three ES clones were expanded and recombinant ES cells injected into C57BL/6J-derived blastocysts that were then implanted into the uteri of recipient females.

Breeding of chimeras and generation of F1 mice heterozygous for the human IGF-1R in the endothelium. Seven highly chimeric males generated by blastocyst injection of ES clones were mated with two wild-type C57BL/6J female mice to examine whether the recombinant ES cells contributed to the germ layer. To assess whether ES cells have contributed to the germ layer of chimeras, mouse coat color markers were used. The ES cells used to develop the model were originally derived from a 129 strain of mice that have an agouti coat color. This marker is dominant over the black coat of C57BL/6 mice. Therefore, mating of the chimeras with C57BL/6J mice should yield agouti-colored pups when the ES cells have contributed to the germ layer. Eight out of 20 agouti F1 females were genotyped by Southern blot. Southern blot validated the correct heterozygous status of eight tested F1 females by detecting the 7.9-kb–sized AvrII fragment of the C57BL/6J *Hprt* wild-type allele and the 9.8-kb–sized AvrII fragment of the reconstituted *Hprt* allele (Fig. 1*B*).

Mice with endothelium-specific deletion of the IGF-1R. To generate mice with endothelium-specific deficiency of the IGF-1R, we used mice carrying a floxed IGF-1R allele (IGF-1RLox) as previously described (15) and mice expressing the cre-recombinase under control of the Tie2 promoter (Tie2 cre; The Jackson Laboratory, Bar Harbor, ME). Male heterozygous Tie2-cre/IGF-1RLox mice were compared with age-matched littermate controls.

Breeding and maintenance of gene-modified mice. hIGFREO mice and mice with endothelium-specific haploinsufficiency of the IGF-1R (ECIGF-1R$^{+/-}$) were bred onto a C57BL/6J background to at least 12 generations. Mice were housed in a conventional animal facility with a 12-h light/dark cycle. Genotyping was performed using ear notch DNA (Fig. 1*C*). Male mice aged 3–5 months were used in all experiments, which were conducted in accordance with accepted standards of humane animal care under United Kingdom Home Office Project license number 40/3523.

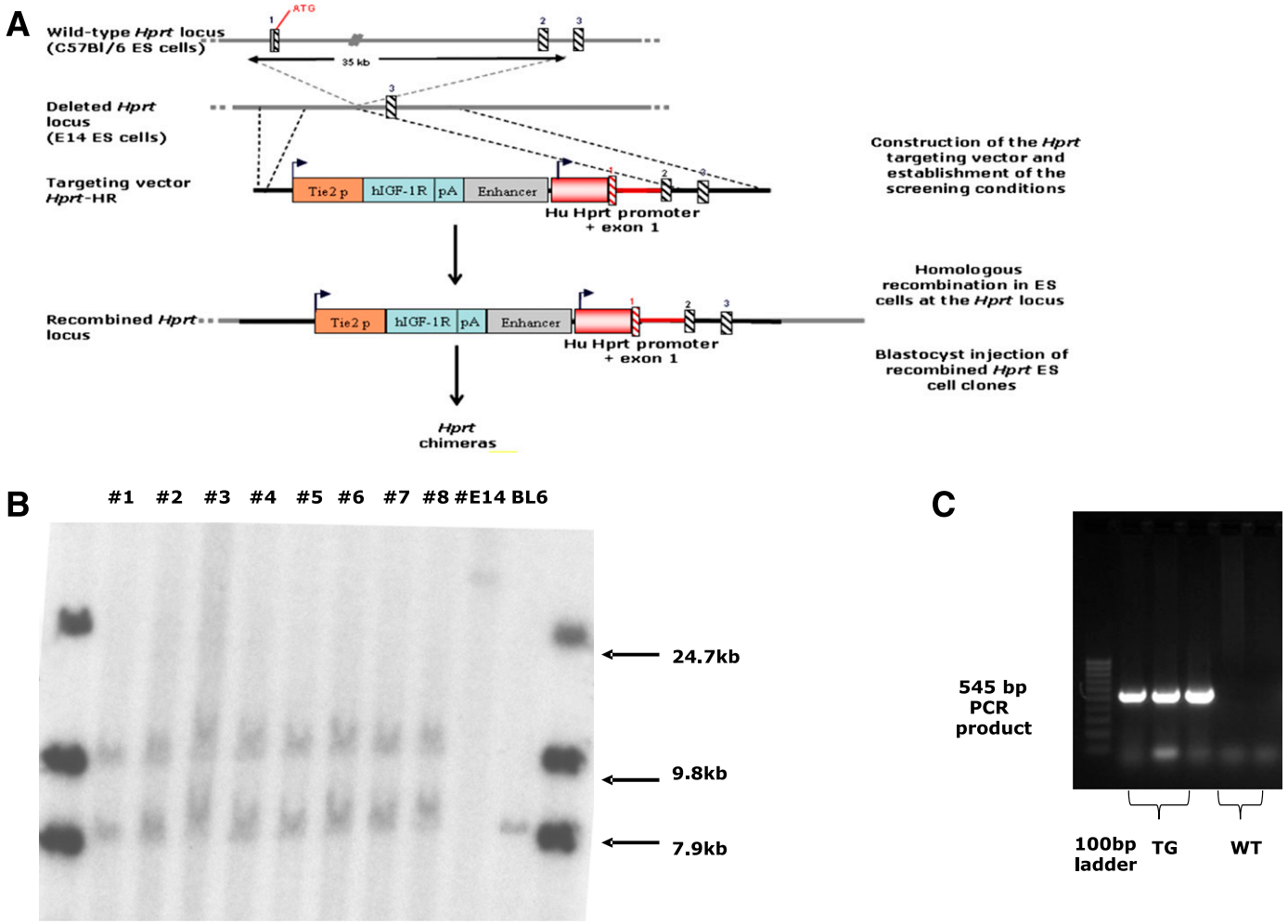

FIG. 1. Generation of transgenic hIGFREO mice using the *Hprt* targeting strategy. *A*: Construction of the *Hprt* targeting vector, homologous recombination in ES cells at the Hprt locus, blastocyst injection of recombined *Hprt* ES cell clones, and generation of chimeras. *B*: Southern blot analysis of the F1 generation. The genomic DNA of the eight F1-tested mice #01-08 was compared with wild-type DNA (E14, BL6). The AvrII-digested DNAs were blotted on nylon membranes and hybridized with a 5′ probe to validate the recombined *Hprt* allele in these animals. The Southern blot validated the correct heterozygous status of eight tested F1 females by detecting the 7.9-kb–sized AvrII fragment of the recombined *Hprt* allele. *C*: Genotyping of transgenic mice with endothelial cell–specific expression of the human IGF-1R. TG, transgenic; WT, wild type. (A high-quality color representation of this figure is available in the online issue.)

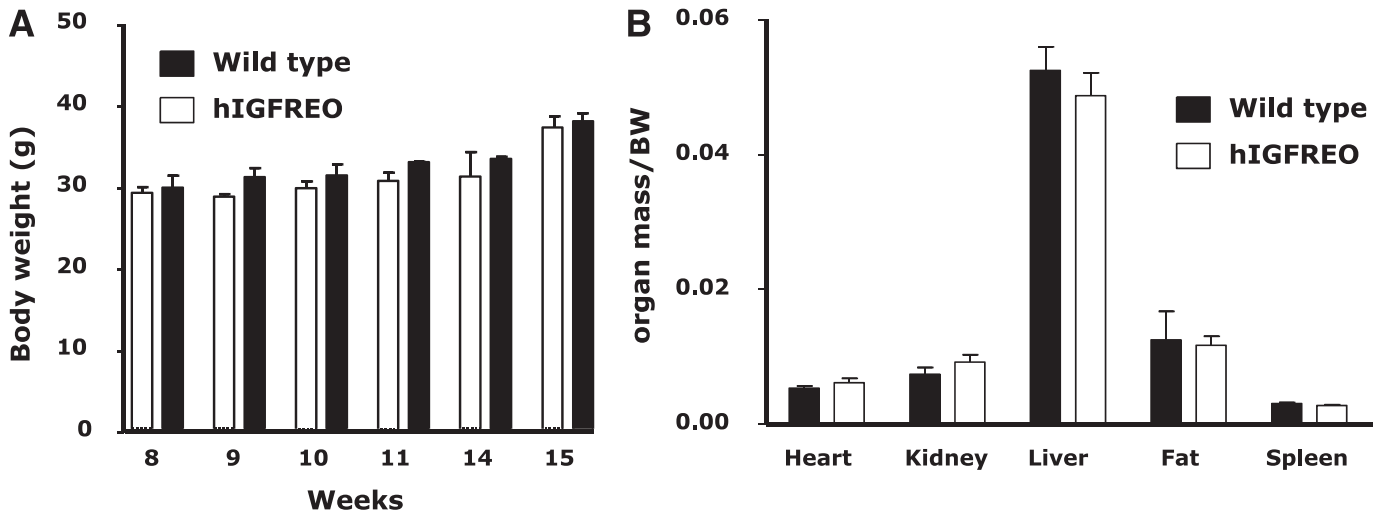

FIG. 2. Growth curves and organ mass of hIGFREO mice. *A*: No difference in growth pattern of hIGFREO mice. *B*: No difference in organ weight of hIGFREO mice. All experiments at least *n* = 6 mice per group. BW, body weight.

Metabolic tests. Glucose, insulin, and IGF-1 tolerance tests were performed by blood sampling after an intraperitoneal injection of glucose, human recombinant insulin, or IGF-1 as previously described (15,20,21). Glucose concentrations were determined in whole blood using a portable meter. Plasma insulin and IGF-1 levels were determined by enzyme-linked immunoassay (20,21).

Studies of vasomotor function in aortic rings. Vasomotor function was assessed ex vivo in aortic rings as previously described (21).

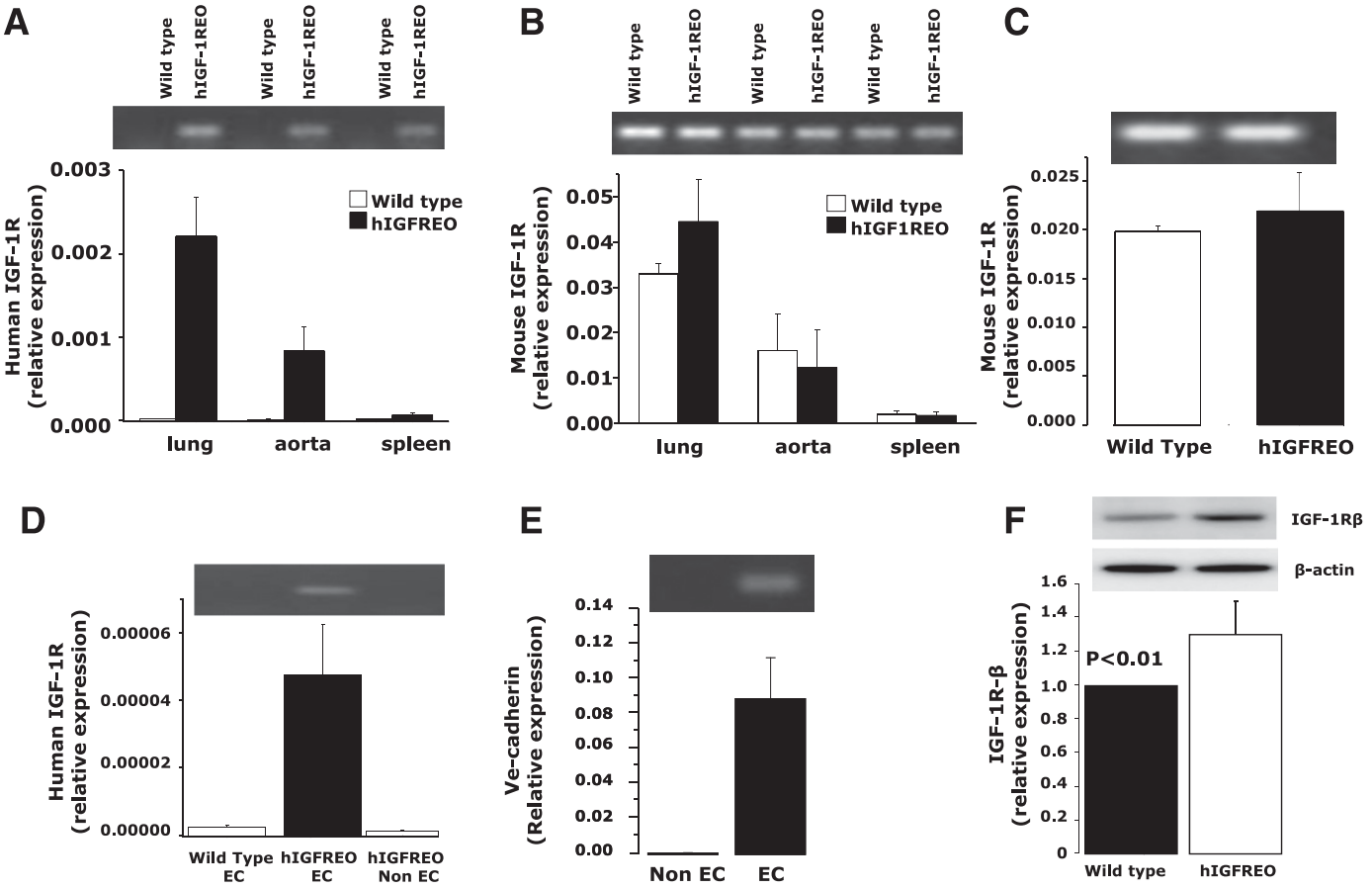

FIG. 3. Characterization of hIGFREO mice. *A*: Expression of human IGF-1R in organs from hIGFREO mice and wild-type littermate controls. *B*: Expression of native (mouse) IGF-1R in organs from hIGFREO mice and wild-type littermate controls. *C*: No difference in murine IGF-1R expression in endothelial cells (EC) from hIGFREO mice compared with wild type. *D*: Expression of human IGF-1R in endothelial cells from hIGFREO mice and no expression in endothelial cells from wild-type mice or nonendothelial cells from hIGFREO mice. *E*: Vascular-endothelial-cadherin (Ve-cadherin) expression in endothelial cells from hIGFREO mice with no expression in nonendothelial cells. *F*: Expression of mouse IGF-1R protein in endothelial cells from hIGFREO mice and wild-type littermates showing significantly greater levels in hIGFREO. All experiments at least *n* = 6 mice per group.

NO synthase activity. After activation, endothelial NO synthase (eNOS) produces NO and L-citrulline in a stoichiometric reaction. The effect of insulin/IGF-1 on eNOS activity in endothelial cells was determined by conversion of [^{14}C]-L-arginine to [^{14}C]-L-citrulline (15,20).

Quantification of eNOS, serine 1177-phosphorylated eNOS, serine-phosphorylated Akt, neuronal NO synthase, IGF-1R, insulin receptor, tyrosine-phosphorylated insulin receptor, and hybrid receptors. Protein expression was quantified in endothelial cells (before and after 10-min exposure to 150 nmol/L insulin or IGF-1) using Western blotting with β-actin as control (15,20,21). Immunoprecipitation of protein for the quantification of hybrid receptors and tyrosine-phosphorylated IR was performed as previously reported (15), incubating equal amounts of protein lysates (100 μg) and 50 μL of protein A-DynaBeads (Invitrogen) precoated with indicated anti-rabbit antibodies for 20 min. After three rounds of washing with PBS/0.01% Tween 20, the beads were resuspended in 2× Laemmli loading buffer supplied with the NOVEX Gel Electrophoresis system (Invitrogen). Aortic protein was separated by SDS-PAGE, and blots were probed with a mouse anti–IGF-1R-α (for hybrid expression), IR-β (C-19), and IGF-1R-β (C-20), antibodies for receptor expression (Santa Cruz Biotechnology), Akt, phosphorylated Akt (pAkt) (21) (Cell Signaling Technology, Beverley, MA), and neuronal NO synthase (nNOS; Transduction Laboratories, Franklin Lakes, NJ). Tyrosine-phosphorylated IR expression was examined in pulmonary endothelial cells (PECs) as we previously reported (15).

Cell lysis, immunoblotting, and immunoprecipitation. Primary cells were lysed in extraction buffer containing (in mmol/L unless otherwise noted): 50 HEPES, 120 NaCl, 1 $MgCl_2$, 1 $CaCl_2$, 10 NaP_2O_7, 20 NaF, 1 EDTA, 10% glycerol, 1% Nonidet P-40, 2 sodium orthovanadate, 0.5 μg/mL leupeptin, 0.2 phenylmethylsulfonyl fluoride, and 0.5 μg/mL aprotinin. Cell extracts were sonicated in an ice bath and centrifuged for 15 min before protein measurements were carried out by BCA assay (Pierce) using the supernatant. Equal amounts of cellular protein were resolved on NuPage 4–12% Bis-Tris gels (Invitrogen) and transferred to polyvinylidene difluoride membranes. Immunoblotting was carried out with indicated primary antibodies. Blots were incubated with appropriate peroxidase-conjugated secondary antibodies and developed with enhanced chemiluminescence (Millipore). Fifty micrograms of total cell lysate was used for immunoprecipitation with indicated antibodies: IR-β (C19; Santa Cruz Biotechnology) and Protein A-DynaBeads (Invitrogen) for 20 min at room temperature. Immune complexes were collected using magnetic field, washed extensively with PBS/0.02% Tween 20, solubilized in Laemmli sample buffer, and analyzed as above. Immunoblots were scanned on a Kodak camera-scanner Image Station 2000R, and bands were quantified using Kodak ID Image Analysis software (Kodak).

Gene expression. mRNA was isolated using a commercial kit (Roche) and the levels of IGF-1R, IR, nNOS, and eNOS mRNA quantified using real-time quantitative PCR (9,15); a range of housekeeping genes were screened for validity and stability prior to measurements (data not shown). Nonspecific primers and those specific for human and mouse IGF-1R were designed and validated in human umbilical vein endothelial cells and mouse pulmonary endothelial cells (PECs) (Supplementary Table 1).

PEC isolation and culture. Primary PECs were isolated from murine lung as we previously described (15).

Fluorescence-based measurement of NO. Insulin- and IGF-1–mediated NO release was measured using 4-amino-5-methylamino-2-difluorofluorescein (DAF-FM) fluorescence (Invitrogen) as we recently described (15).

Femoral artery endothelial denuding arterial injury and en face microscopy. Femoral artery wire injury was performed as we previously reported (10). Mice were anesthetized at 5 days after wire injury and 50 mL of 5% Evans blue dye injected into the vena cava. The mice were perfused/fixed with formaldehyde before femoral arteries (injured and uninjured) were harvested. The vessels were opened longitudinally. The areas stained and unstained in blue were measured in the injured area 5 mm from the proximal suture and the percentage areas calculated using ImagePro Plus 6.0 software (Media Cybernetics, Bethesda, MD).

Endothelial cell migration. PECs were suspended in supplemented basal medium. Approximately 4 × 10^4 cells in 500 μL MV2 medium (PromoCell, Heidelberg, Germany) were placed in the upper compartment of a Modified Boyden chamber with a polycarbonate membrane containing 8 μm pores. The lower compartment contained 750 μL MV2 and 50 ng/ml vascular endothelial growth factor (VEGF165); negative control wells contained basal MV2 medium (vehicle) alone. Wells were set up in triplicate and incubated in 5% CO_2 at 37°C for 24 h. Membranes were fixed in 70% ethanol at −20°C for 1 h before

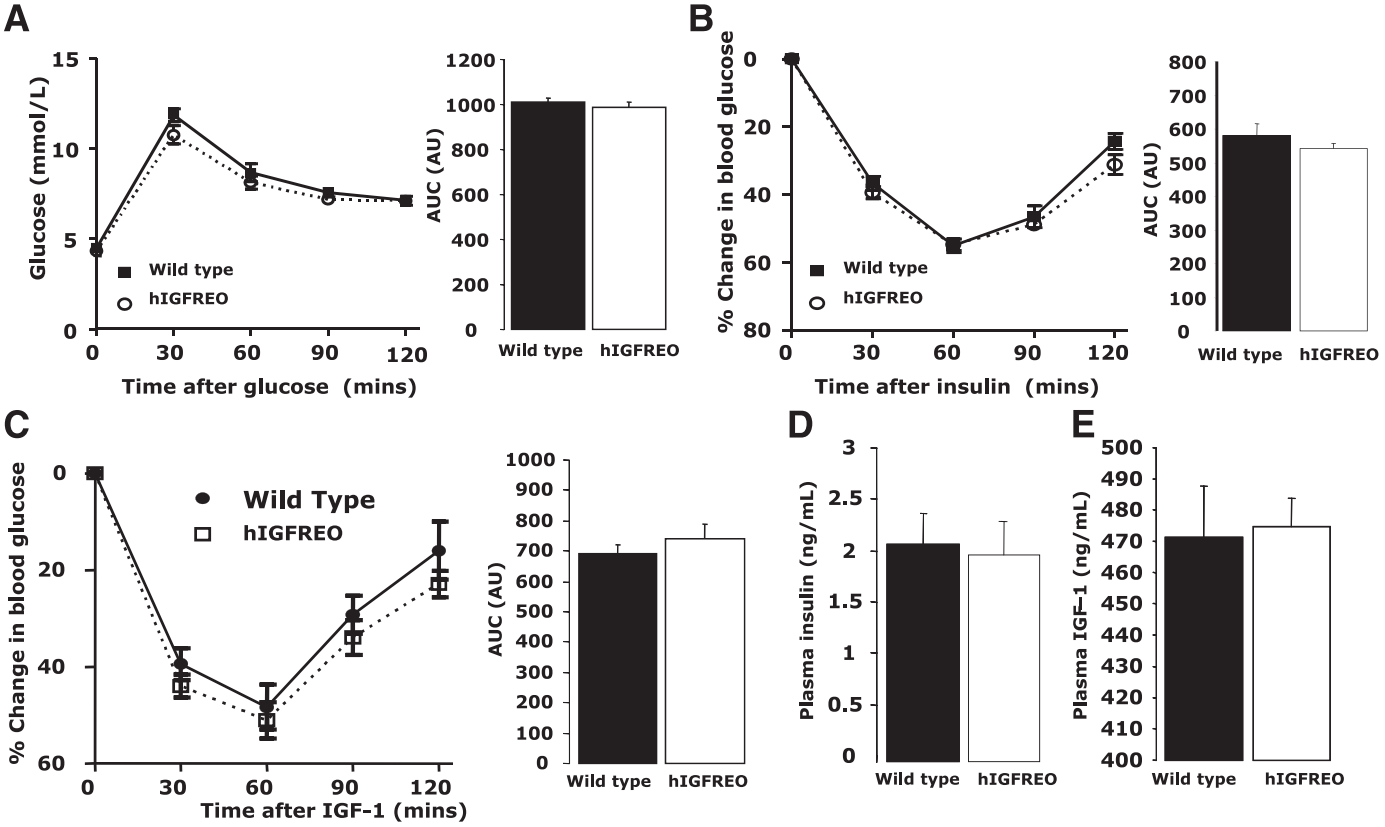

FIG. 4. Metabolic function in hIGFREO mice. Increasing endothelium IGF-1R has no effect on glucose tolerance or insulin sensitivity. *A*: Glucose tolerance tests. *B*: Insulin tolerance tests. *C*: IGF-1 tolerance tests. *D*: Fasting insulin. *E*: Fasting IGF-1. All experiments at least *n* = 10 mice per group. (Area under the curve [AUC] represents absolute change in glucose.)

mechanical removal of cells adherent to the upper surface using a cotton swab. Hematoxylin and eosin stains were then applied (30 s each) to membranes that were then washed in water and mounted on glass slides. Migrant PECs were counted in 10 high-power fields (×200 magnification, area of 720 × 530 μm). Results expressed as mean cell number per high-power field.

Endothelial progenitor cell isolation. Endothelial progenitor cells (EPC) were isolated from bone marrow and spleen as we previously reported (10).

Statistics. Results are expressed as mean (SEM). Comparisons within groups were made using paired Student *t* tests and between groups using unpaired Student *t* tests or repeated-measures ANOVA, as appropriate; when repeated *t* tests were performed, a Bonferroni correction was applied. A P value <0.05 was considered statistically significant.

RESULTS

Generation and characterization of transgenic hIGFREO mice. We generated a novel hIGFREO mouse (Figs. 1–3). hIGFREO mice were born with the same frequency as wild-type mice. There was no difference in behavior, grooming, growth (Fig. 2*A*), or organ weight (Fig. 2*B*). We determined the levels of human and native (mouse) IGF-1R mRNA expression in organs with different proportions of endothelial cells (lung, aorta, and spleen). Human IGF-1R mRNA expression was approximately threefold higher in lung than in aorta from hIGFREO; $P < 0.01$ (Fig. 3*A*). In spleen, there was very little IGF-1R, commensurate with proportionately fewer endothelial cells. Human IGF-1R expression in hIGFREO mice tracked the pattern for native IGF-1R seen in wild-type mice (Fig. 3*B*). There was no difference in expression of mouse IGF-1R between hIGFREO and wild type (Fig. 3*C*). There was no hIGF-1R mRNA detectable in endothelial cells from wild-type mice or nonendothelial cells from hIGFREO mice (Fig. 3*D*); nonendothelial cells did not express the endothelial-specific marker vascular-endothelial-cadherin in contrast to endothelial cells (Fig. 3*E*). Western blot analysis confirmed that total IGF-1R protein levels were significantly increased in hIGFREO endothelial cells compared with wild type (Fig. 3*F*).

hIGFREO mice have normal glucose homeostasis. hIGFREO had similar responses to insulin, glucose, and IGF-1 tolerance tests as wild-type mice (Fig. 4*A*–*C*). Fasting glucose (4.4 [0.3] versus 4.5 [0.3] mmol/L; P = NS), insulin (hIGFREO 2.0 [0.3] versus wild-type 2.1 [0.3] ng/ml; P = NS), and IGF-1 (hIGFREO 474 [31] versus wild-type 471 [16] ng/ml; P = NS) were similar in hIGFREO and wild-type mice (Fig. 4*D* and *E*).

hIGFREO increases hybrid receptors but has no effect on eNOS expression, aortic relaxation in response to IGF-1, or eNOS activation in response to IGF-1. There were no differences in endothelial cell or lung eNOS mRNA (Fig. 5A). In keeping with our previous report (15),

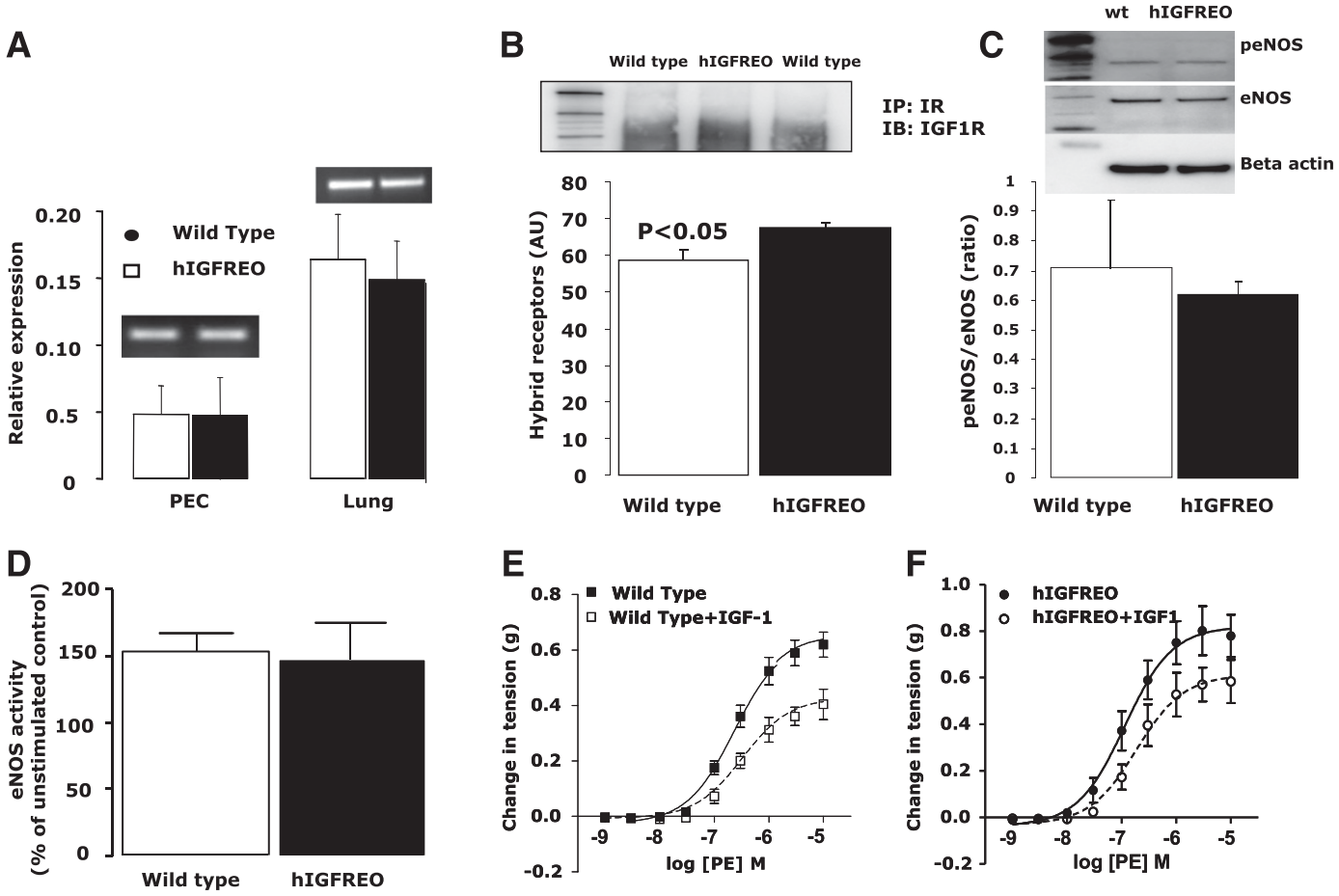

FIG. 5. hIGFREO mice have similar eNOS mRNA in endothelial cells and lung tissue. hIGFREO mice have increased hybrid receptors, similar serine 1177-phosphorylated eNOS protein expression, and similar aortic relaxation and eNOS activation in response to IGF-1 as wild-type littermates. *A*: No differences in endothelial cell or lung eNOS mRNA from hIGFREO mice compared with wild-type littermates. *B*: Increased hybrid receptors in endothelial cells from hIGFREO mice. *C*: No differences in serine-phosphorylated eNOS protein concentration in endothelial cells from hIGFREO mice. *D*: No difference in eNOS activation in response to IGF-1 in hIGFREO mice. *E*: Aortic relaxation responses in hIGFREO mice in response to IGF-1. *F*: Aortic relaxation responses in wild-type littermates (all experiments at least *n* = 6 mice per group).

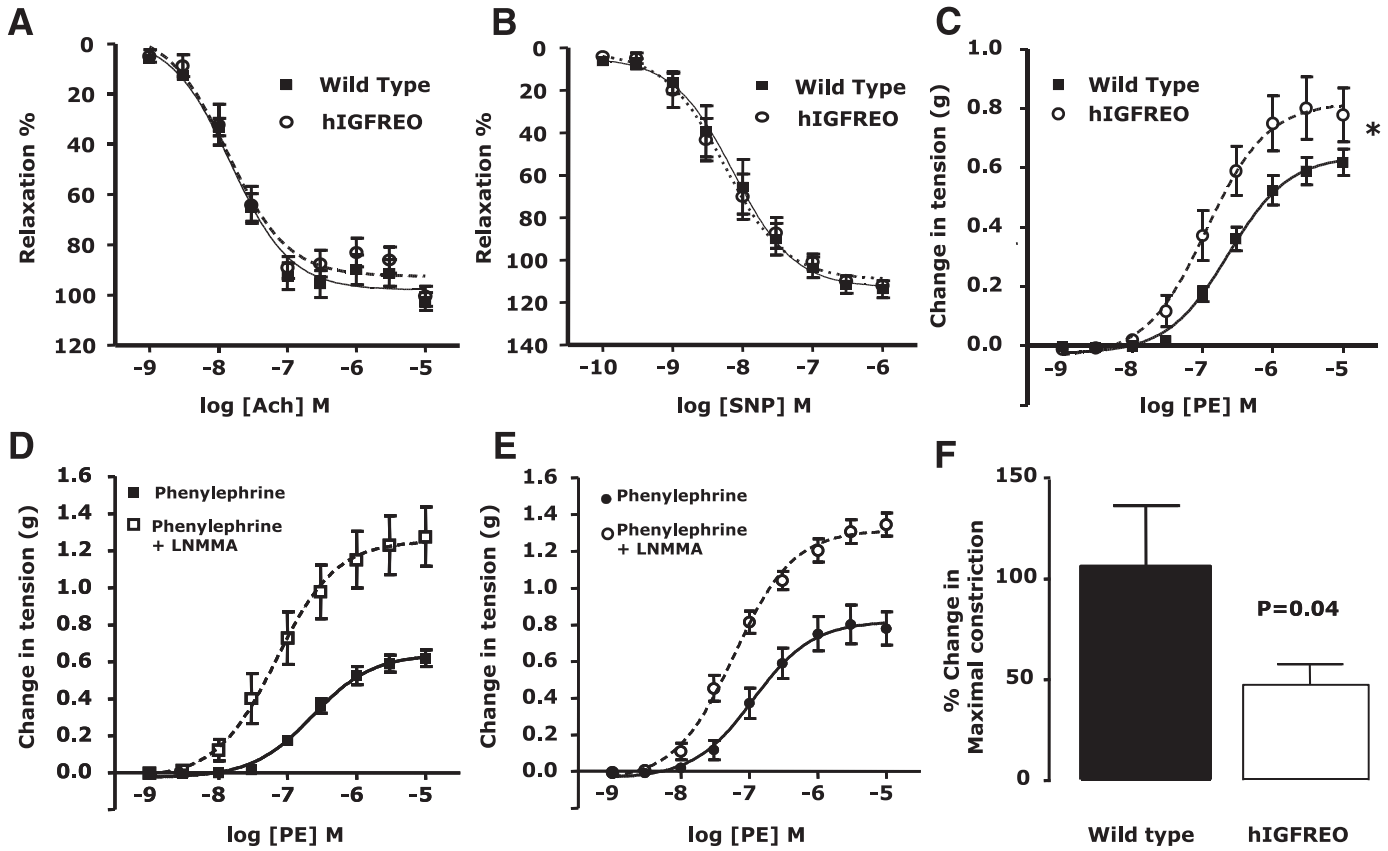

FIG. 6. Endothelial function in hIGFREO mice. *A*: Acetylcholine relaxation responses are similar in hIGFREO mice compared with wild-type littermates. *B*: Single nucleotide polymorphism (SNP) relaxation responses are similar in hIGFREO mice compared with wild-type littermates. *C*: Phenylephrine constriction curves demonstrating enhanced constriction to phenylephrine in hIGFREO mice. *D*: Constriction to L-NMMA in wild-type mice. *E*: Constriction to L-NMMA in hIGFREO mice indicative of reduced basal NO bioavailability compared with wild-type mice. *F*: Maximal constriction to L-NMMA in hIGFREO mice and wild-type littermates. All experiments at least $n = 6$ mice per group. *$P < 0.05$.

insulin-resistant hybrid receptors were increased in endothelial cells from hIGFREO mice (Fig. 5*B*); there was no difference in IR-β or tyrosine-phosphorylated IR-β expression between hIGFREO and wild-type littermates (Supplementary Fig. 1). Basal serine 1177 eNOS phosphorylation (Fig. 5*C*), eNOS activation (Fig. 5*D*), and aortic ring relaxation responses (Fig. 5*E* and *F*) in response to IGF-1 were no different when comparing hIGFREO mice and wild-type mice. Insulin-mediated aortic relaxation in hIGFREO mice was no different than wild-type mice (data not shown). IGF-1–stimulated 1177 serine phosphorylation of eNOS was similar in endothelial cells from hIGFREO and wild-type mice (Supplementary Figs. 2 and 3).

hIGFREO mice have increased constrictor responses to phenylephrine, reduced basal NO bioavailability, and normal responses to acetylcholine and sodium nitroprusside. There were no differences in aortic ring relaxation responses to acetylcholine or SNP between mice (Fig. 6*A* and *B*). In contrast to this, hIGFREO mice had enhanced constrictor responses to phenylephrine (Fig. 6*C*), and consistent with reduced basal NO bioavailability, a blunted constrictor response to N^G-monomethyl-L-arginine (L-NMMA) (Fig. 6*D–F*).

hIGFREO mice have similar arterial blood pressure as wild-type littermates. Trained, semirestrained hIGFREO mice had systolic blood pressure of 106.7 (3.0) mmHg compared with wild-type littermates 105.8 (4.5) mmHg; $P = 0.8$ (Fig. 7*A*).

hIGFREO mice have reduced insulin-stimulated eNOS serine 1177 phosphorylation, reduced insulin-stimulated eNOS activity, and reduced insulin-stimulated NO production in endothelial cells. Insulin-mediated NO release (Fig. 7*B* and *C*), eNOS activation (Fig. 7*D*), and eNOS serine 1177 phosphorylation (Fig. 7*E*) were blunted in hIGFREO endothelial cells compared with wild type.

hIGFREO mice have reduced neuronal NO synthase protein expression in endothelial cells. Recent studies provide compelling evidence for a role for nNOS-derived NO in basal vascular tone (22). We therefore measured nNOS mRNA and protein expression in endothelial cells from wild-type and hIGFREO mice. There was no difference nNOS mRNA expression (data not shown), whereas protein expression was reduced approximately twofold in hIGFREO mice (Supplementary Fig. 4).

hIGFREO mice have enhanced endothelial cell migration and accelerated endothelial regeneration after arterial injury. Endothelium regeneration after wire injury (Fig. 8*A*) was significantly enhanced in hIGFREO mice compared with wild-type mice (percent recovered area wild type 57% [2%] versus hIGFREO 47% [5%]; $P < 0.05$). Consistent with enhanced in situ endothelium regeneration, migration to control and VEGF was substantially enhanced in endothelial cells from hIGFREO mice (Fig. 8*B*). To further examine the role of the IGF-1R in endothelial regeneration after denuding arterial injury, we performed complementary wire injury experiments in ECIGF-1R$^{+/-}$ mice and assessed

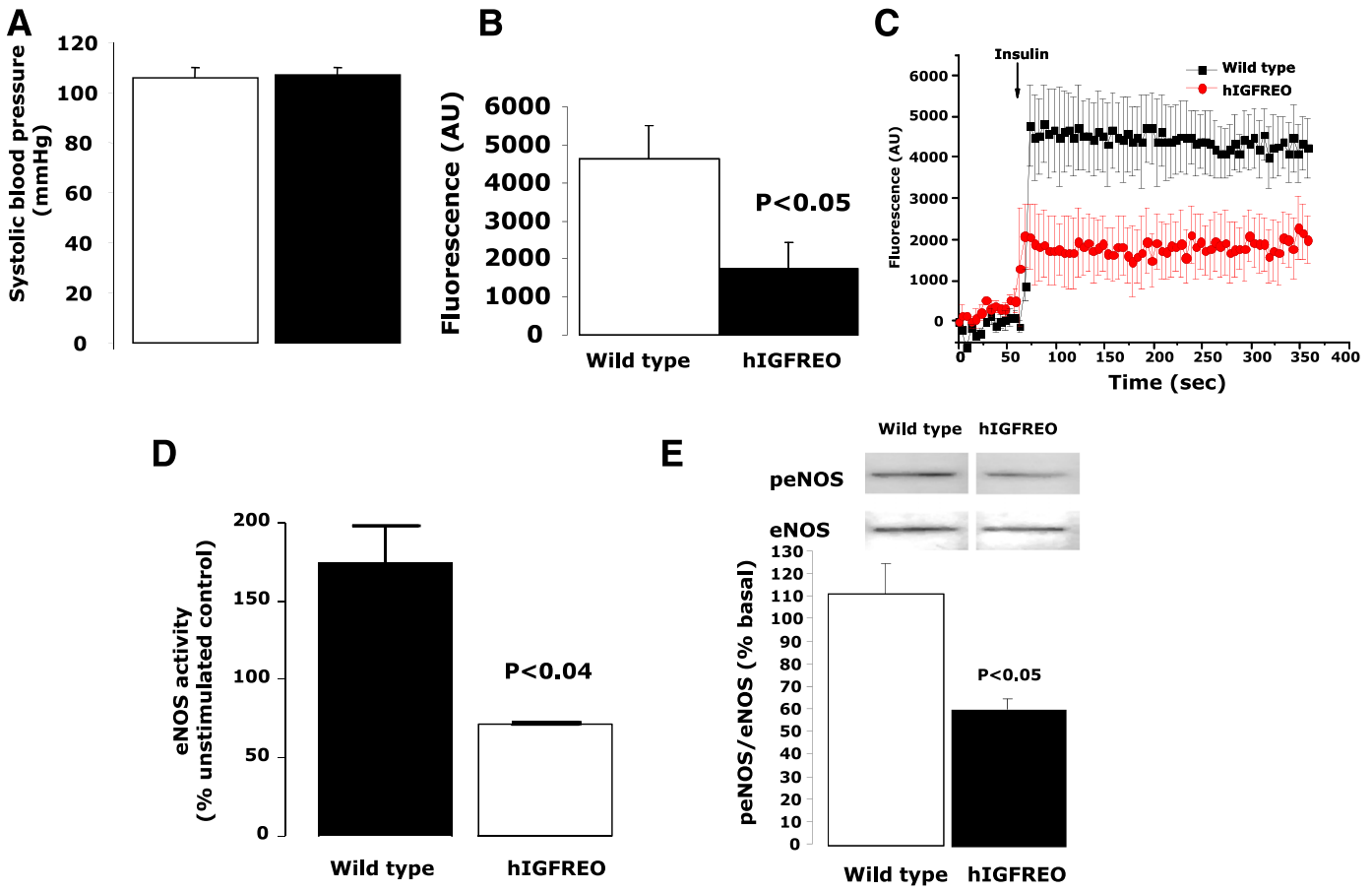

FIG. 7. Systolic blood pressure, insulin-stimulated eNOS phosphorylation, eNOS activation, and NO production in endothelial cells from hIGFREO mice. *A*: Systolic blood pressure is similar in hIGFREO mice and wild-type littermates. *B*: Insulin-mediated NO release in endothelial cells from wild-type mice and hIGFREO mice showing blunted responses in hIGFREO mice. *C*: Representative time-series graph for change of DAF-FM fluorescence (Invitrogen) in PECs in response to insulin (100 nmol/L). *D*: eNOS activity in response to insulin in endothelial cells from hIGFREO and wild-type mice showing blunted responses in hIGFREO mice. *E*: Serine 1177 phosphorylation of eNOS in endothelial cells in response to insulin is blunted in hIGFREO mice compared with wild-type littermate mice. All experiments at least $n = 6$ mice per group. (A high-quality color representation of this figure is available in the online issue.)

regeneration. Consistent with our findings in hIGFREO mice, ECIGF-1R$^{+/-}$ mice had blunted endothelium regeneration when compared with wild-type littermates (percent recovered at 5 days, ECIGF-1R$^{+/-}$ 26% (1%) versus wild-type 42% (1%); $P < 0.01$) (Fig. 8*C*). We examined the expression of hIGF-1R in spleen and bone marrow-derived EPC, and hIGF-1R was expressed in EPC from hIGFREO but not wild type (Supplementary Fig. 5).

DISCUSSION

In this study, we describe the phenotype of a novel transgenic mouse with endothelium-targeted expression of the human IGF-1R generated to investigate the role of the IGF-1R in regulating endothelial cell function. The major findings of this study are as follows: *1*) endothelial-specific IGF-1R overexpression leads to an increase in total IGF-1R mRNA and protein in hIGFREO mice compared with wild-type littermates; *2*) endothelial IGF-1R overexpression is associated with an increase in vasoconstrictor responsiveness to phenylephrine, reduced basal NO release, and reduced nNOS expression; *3*) the IGF-1R is a potent negative regulator of insulin-mediated NO release; and *4*) despite this reduced NO bioavailability, endothelial IGF-1R overexpression leads to enhanced endothelium regeneration after denuding wire injury.

The IGF-1R is a negative regulator of insulin sensitivity and NO bioavailability in the endothelium. We recently demonstrated that global haploinsufficiency of the IGF-1R enhances whole-body insulin sensitivity and insulin-mediated NO production (15) and knocking down IGF-1R in human endothelial cells enhanced basal and insulin-stimulated serine-phosphorylated eNOS. In mice with endothelium-specific knockdown of the IGF-1R, we confirmed a gene-dose response effect on basal NO bioavailability. Moreover, by crossing IGF-1R haploinsufficient mice with IR-haploinsufficient mice (IR$^{+/-}$), we were able to restore insulin-mediated NO release in IR$^{+/-}$ mice. We also showed that reducing IGF-1R density altered IGF-1R–IR stoichiometry in favor of IR holoreceptors with a relative reduction in insulin-resistant hybrid receptors.

In the present report, we demonstrate that increasing IGF-1R numbers specifically in the endothelium has no effect on the response to systemic insulin, IGF-1, or glucose. Despite having no effect on whole-body glucose homeostasis, IGF-1R overexpression led to reduced insulin-stimulated eNOS serine phosphorylation, eNOS activation, and NO generation. Overexpression of the IGF-1R also reduced basal NO bioavailability. Reduced NO has been shown to promote the development of atherosclerosis (23,24). Serine phosphorylation increases eNOS calcium sensitivity and augments NO biosynthesis and release (25); consistent with

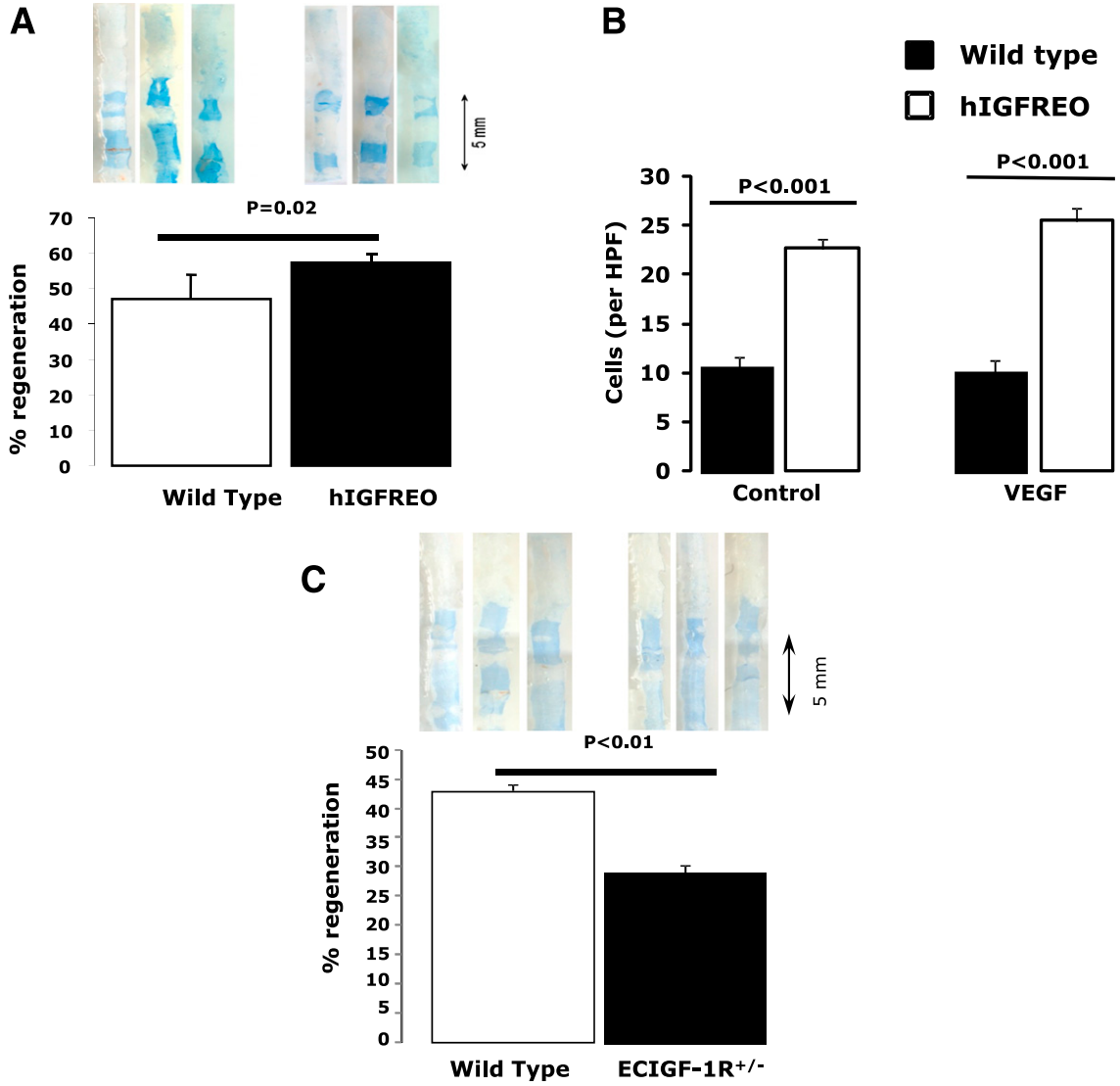

FIG. 8. hIGFREO mice have enhanced endothelial cell migration in vitro and accelerated endothelial repair after denuding femoral artery wire injury. *A*: Endothelial regeneration in hIGFREO mice and wild-type littermates after wire injury showing enhanced endothelial regeneration in hIGFREO mice. *B*: Migration to VEGF and control media is enhanced in PECs from hIGFREO mice. *C*: Endothelial regeneration in wild-type and ECIGF-1R$^{+/-}$ mice after wire injury showing blunted regeneration in ECIGF-1R$^{+/-}$ mice. All experiments at least *n* = 6 mice per group. HPF, high-power field. (A high-quality color representation of this figure is available in the online issue.)

this, eNOS phosphorylation status has been shown to play an important and favorable role in a range of pathological situations reminiscent of human vascular disease (26,27). Our dataset demonstrates that a relative increase in IGF-1R in relation to IR, which is a hallmark of type 2 diabetes (28,29), has an unfavorable impact on NO bioavailability.

The IGF-1R has pathway-selective effects on eNOS activation. eNOS can be activated by a range of different stimuli. Fluid shear stress and growth factors such as insulin activate eNOS via phosphatidylinositol 3-kinase and Akt/protein kinase B activation in what is often described as a calcium-independent fashion (25). Secondly, different agonists (such as acetylcholine) activate eNOS by stimulating a rise in intracellular calcium, described as calcium-dependent eNOS activation (30). In the present report, we have shown that the IGF-1R selectively inhibits insulin-mediated eNOS activation with preservation of acetylcholine responses. Interestingly, hIGFREO mice had a relative reduction in endothelial cell expression of nNOS, possibly contributing to reduced basal NO bioavailability.

hIGFREO, glucose homeostasis, growth, and metabolism. Endothelial cell-specific overexpression of the IGF-1R had no effect on growth, whole body, or organ weight. In contrast to a recent report (31), the endothelial cell insulin resistance demonstrated in the present report had no effect on whole-body glucose uptake. The mechanisms underlying the difference between mice with endothelium-specific deletion of IR substrate-2 described by Kubota et al. (31) and hIGFREO mice are unclear. It may be that insulin resistance in the endothelium due to perturbation of insulin signaling at its most proximal signaling node (i.e., the IR), as seen in this report, our previous study (11), and that of Vicent et al. (32), does not affect insulin sensitivity in skeletal muscle. These data highlight the complexity of communication between different cell types involved in insulin signaling.

The IGF-1R enhances endothelium regeneration. It is now a well-accepted paradigm that cardiovascular risk factors lead to damage/death of resident endothelial cells, and endogenous repair mechanisms are activated to repair

the damage (for review, see Ref. 33). Intriguingly and despite reduced NO bioavailability, overexpression of the human IGF-1R in the endothelium accelerated repair of the endothelium after wire injury. Recent data demonstrate that repair of denuded endothelium is principally a result of elongation, growth, and migration of resident endothelial cells (34). The present dataset is compatible with this paradigm, showing enhanced migration of endothelial cells from hIGFREO mice.

More recently, it has emerged that bone marrow or other tissue-derived EPC may contribute to endothelial repair (33). We have demonstrated that insulin-resistant humans (35) and mice (10) have impairment of EPC mobilization and function. Studies have shown that IGF-1 may have favorable effects on EPC function and numbers in humans (36) and mice (37). Our dataset demonstrating the expression of the human IGF-1R in EPC from hIGFREO mice but not wild type and the enhanced endothelium repair after injury raises the possibility that increasing IGF-1R expression may have an effect on EPC function, and this warrants further studies.

Perspective. In the present dataset and our recent report (15), we have demonstrated that within a tight and physiologically relevant range, the IGF-1R plays a critical role in regulating basal NO bioavailability and insulin-mediated NO release. We have also shown a novel role for the IGF-1R in regulation of nNOS and that the effect of the IGF-1R appears to be specific to insulin-mediated NO release.

Despite leading to reduced basal and insulin-stimulated NO release, increasing IGF-1R enhances endothelial repair. This provides a compelling portfolio of evidence supporting an important role for IGF-1R within a (patho)physiological range in regulating NO bioavailability and vascular repair. Many human diseases are characterized by excessive or impaired tissue growth and vascularization. The present dataset and our previous report (15) establish the manipulation of IGF-1R: insulin receptor stoichiometry as a novel approach to regulating NO bioavailability and a potential treatment for disorders of excessive or impaired vascular growth and repair. Examining how hybrid formation is regulated and whether or not the human IGF-1R behaves differently to mouse IGF-1R in hybrid formation warrant future work.

ACKNOWLEDGMENTS

This work was supported by the British Heart Foundation and Medical Research Council, U.K.

No potential conflicts of interest relevant to this article were reported.

H.I., H.V., P.S., A.A., R.M.C., N.Y., M.G., J.S., S.G., A.S., S.T.R., T.S.F., and V.K.G. performed experiments and analyzed data. S.X., P.J.G., K.M.C., D.J.B., and S.B.W. contributed to discussion and reviewed and edited the manuscript. M.T.K. wrote the manuscript. K.M.C., D.J.B., S.B.W., and M.T.K. obtained funding and designed experiments. M.T.K. is the guarantor of this work and, as such, had full access to all the data in the study and takes responsibility for the integrity of the data and the accuracy of the data analysis.

REFERENCES

1. Razani B, Semenkovich CF. Getting away from glucose: stop sugarcoating diabetes. Nat Med 2009;15:372–373
2. Booth GL, Kapral MK, Fung K, Tu JV. Relation between age and cardiovascular disease in men and women with diabetes compared with non-diabetic people: a population-based retrospective cohort study. Lancet 2006;368:29–36
3. Marso SP, Hiatt WR. Peripheral arterial disease in patients with diabetes. J Am Coll Cardiol 2006;47:921–929
4. Stegmayr B, Asplund K. Diabetes as a risk factor for stroke. A population perspective. Diabetologia 1995;38:1061–1068
5. Reiber GE, Boyko EJ, Smith DG. Lower extremity foot ulcers and amputations in diabetes. In *Diabetes in America*. Harris MI, Stern MP, Eds. Bethesda, Maryland, U.S. Government Printing Office, 1995, p. 409–428
6. Kempen JH, O'Colmain BJ, Leske MC, et al.; Eye Diseases Prevalence Research Group. The prevalence of diabetic retinopathy among adults in the United States. Arch Ophthalmol 2004;122:552–563
7. Nakagawa T, Kosugi T, Haneda M, Rivard CJ, Long DA. Abnormal angiogenesis in diabetic nephropathy. Diabetes 2009;58:1471–1478
8. Muniyappa R, Montagnani M, Koh KK, Quon MJ. Cardiovascular actions of insulin. Endocr Rev 2007;28:463–491
9. Wheatcroft SB, Shah AM, Li JM, et al. Preserved glucoregulation but attenuation of the vascular actions of insulin in mice heterozygous for knockout of the insulin receptor. Diabetes 2004;53:2645–2652
10. Kahn MB, Yuldasheva NY, Cubbon RM, et al. Insulin resistance impairs circulating angiogenic progenitor cell function and delays endothelial regeneration. Diabetes 2011;60:1295–1303
11. Duncan ER, Crossey PA, Walker S, et al. Effect of endothelium-specific insulin resistance on endothelial function in vivo. Diabetes 2008;57:3307–3314
12. De Meyts P, Whittaker J. Structural biology of insulin and IGF1 receptors: implications for drug design. Nat Rev Drug Disc 2002;1:769–783
13. Slaaby R, Schäffer L, Lautrup-Larsen I, et al. Hybrid receptors formed by insulin receptor (IR) and insulin-like growth factor I receptor (IGF-IR) have low insulin and high IGF-1 affinity irrespective of the IR splice variant. J Biol Chem 2006;281:25869–25874
14. Gatenby V, Kearney MT. Targeting vascular IGF-1 resistance in obesity and type 2 diabetes mellitus. Expert Opin Ther Targets 2010;14:1333–1342
15. Abbas A, Imrie H, Viswambharan H, et al. The insulin-like growth factor-1 receptor is a negative regulator of nitric oxide bioavailability and insulin sensitivity in the endothelium. Diabetes 2011;60:2169–2178
16. Guillot PV, Liu L, Kuivenhoven JA, Guan J, Rosenberg RD, Aird WC. Targeting of human eNOS promoter to the Hprt locus of mice leads to tissue-restricted transgene expression. Physiol Genomics 2000;2:77–83
17. Minami T, Kuivenhoven JA, Evans V, Kodama T, Rosenberg RD, Aird WC. Ets motifs are necessary for endothelial cell-specific expression of a 723-bp Tie-2 promoter/enhancer in Hprt targeted transgenic mice. Arterioscler Thromb Vasc Biol 2003;23:2041–2047
18. Bendall JK, Rinze R, Adlam D, et al. Endothelial Nox2 overexpression potentiates vascular oxidative stress and hemodynamic response to angiotensin II: studies in endothelial-targeted Nox2 transgenic mice. Circ Res 2007;100:1016–1025
19. Li S, Ferber A, Miura M, Baserga R. Mitogenicity and transforming activity of the insulin-like growth factor-I receptor with mutations in the tyrosine kinase domain. J Biol Chem 1994;269:32558–32564
20. Imrie H, Abbas A, Viswambharan H, et al. Vascular insulin-like growth factor-I resistance and diet-induced obesity. Endocrinology 2009;150:4575–4582
21. Rajwani A, Ezzat V, Smith J, et al. Increasing Circulating IGFBP1 Levels Improves Insulin Sensitivity, Promotes Nitric Oxide Production, Lowers Blood Pressure, and Protects Against Atherosclerosis. Diabetes 2012;61:915–924
22. Seddon M, Melikian N, Dworakowski R, et al. Effects of neuronal nitric oxide synthase on human coronary artery diameter and blood flow in vivo. Circulation 2009;119:2656–2662
23. Bugiardini R, Manfrini O, Pizzi C, Fontana F, Morgagni G. Endothelial function predicts future development of coronary artery disease: a study of women with chest pain and normal coronary angiograms. Circulation 2004;109:2518–2523
24. Chen J, Kuhlencordt PJ, Astern J, Gyurko R, Huang PL. Hypertension does not account for the accelerated atherosclerosis and development of aneurysms in male apolipoprotein e/endothelial nitric oxide synthase double knockout mice. Circulation 2001;104:2391–2394
25. Fulton D, Gratton JP, McCabe TJ, et al. Regulation of endothelium-derived nitric oxide production by the protein kinase Akt. Nature 1999;399:597–601
26. Atochin DN, Wang A, Liu VW, et al. The phosphorylation state of eNOS modulates vascular reactivity and outcome of cerebral ischemia in vivo. J Clin Invest 2007;117:1961–1967
27. Schleicher M, Yu J, Murata T, et al. The Akt1-eNOS axis illustrates the specificity of kinase-substrate relationships in vivo. Sci Signal 2009;2:ra41
28. Jiang ZY, Lin YW, Clemont A, et al. Characterization of selective resistance to insulin signaling in the vasculature of obese Zucker (fa/fa) rats. J Clin Invest 1999;104:447–457

29. Federici M, Porzio O, Zucaro L, et al. Increased abundance of insulin/IGF-I hybrid receptors in adipose tissue from NIDDM patients. Mol Cell Endocrinol 1997;135:41–47
30. Bredt DS, Hwang PM, Glatt CE, Lowenstein C, Reed RR, Snyder SH. Cloned and expressed nitric oxide synthase structurally resembles cytochrome P-450 reductase. Nature 1991;351:714–718
31. Kubota T, Kubota N, Kumagai H, et al. Impaired insulin signaling in endothelial cells reduces insulin-induced glucose uptake by skeletal muscle. Cell Metab 2011;13:294–307
32. Vicent D, Ilany J, Kondo T, et al. The role of endothelial insulin signaling in the regulation of vascular tone and insulin resistance. J Clin Invest 2003; 111:1373–1380
33. Cubbon RM, Ali N, Sengupta A, Kearney MT. Insulin- and growth factor-resistance impairs vascular regeneration in diabetes mellitus. Curr Vasc Pharmacol 2012;10:271–284
34. Itoh Y, Toriumi H, Yamada S, Hoshino H, Suzuki N. Resident endothelial cells surrounding damaged arterial endothelium reendothelialize the lesion. Arterioscler Thromb Vasc Biol 2010;30:1725–1732
35. Cubbon RM, Murgatroyd SR, Ferguson C, et al. Human exercise-induced circulating progenitor cell mobilization is nitric oxide-dependent and is blunted in South Asian men. Arterioscler Thromb Vasc Biol 2010;30:878–884
36. Thum T, Hoeber S, Froese S, et al. Age-dependent impairment of endothelial progenitor cells is corrected by growth-hormone-mediated increase of insulin-like growth-factor-1. Circ Res 2007;100: 434–443
37. Sukhanov S, Higashi Y, Shai SY, et al. IGF-1 reduces inflammatory responses, suppresses oxidative stress, and decreases atherosclerosis progression in ApoE-deficient mice. Arterioscler Thromb Vasc Biol 2007;27: 2684–2690